A digital control strategy of high-frequency link inverter with matrix convertor

Yunbo Gao

School of Automation & Electrical Engineering,
Lanzhou Jiaotong University, Lanzhou 730070, Gansu, China

Pengwu Han

Beijing Aerospace Long March Scientific and Technical Information Institute,
Beijing 100076, Beijing, China

Abstract
According to the topology of high-frequency link inverter with matrix converter, a control strategy of separation and link has been proposed to safely convert current in matrix convertor. Based on the polarity of the output side of voltage waveform for high-frequency transformer, the matrix converter is equivalent to two conventional three-phase inverters. Thus, the control strategy of traditional three-phase inverter can be introduced into the matrix converter. Compared with the traditional strategy of converting current of matrix convertor, the control strategy based on separation and link is easy to implement and analyze the working principles. Two PWM signals with opposite phase and three SPWM signals with phase difference of 120° can be produced by DSP. After the logic operation of CPLD, 12 switch signals can be produced to control matrix converter. The results of simulation with Matlab/simulink and experiments show that the proposed control strategy is valid.
Key words: SEPARATION AND LINK, MATRIX CONVERTER, HIGH-FREQUENCY LINK, INVERTER, DSP & CPLD

1. Introduction

The inverters are widely used in various industries, such as power distribution system in aviation, airplanes, radar, and power generation of new energy and so on. The conversion process of high-frequency link inverter with matrix convertor can be described that 25V DC power supply can be translated into rectangular high-frequency voltage through full-bridge inverter circuits, which is modulated by matrix converter, then the sinusoidal voltage with constant-voltage and constant-frequency will be output by filter.

The kernel of power supply in aviation is inverter, which should have the ability to output high-quality voltage waveform, in special applications it requires high stability, enough output power and small size [1]. In 1997, Mr. Espelage and Mr. Bose proposed a new concept of high-frequency link inverter technology [2]. After that, the three-phase high-frequency link inverter technology

has been widely used for small size, light weight, high power density, adjustable power factor, high reliability, etc [3-7]. Due to its convenience in application, more and more researches based on high-frequency link converter technology have got a lot of new achievements [8-13]. Directing at three-phase/single-phase matrix converter system, literature [3] proposes a method of average voltage pulse width modulation (PWM), considering the particular leakage current characteristic of RB-IGBT, it also proposes a method of two-step commutation suitable for RB-IGBT based on the input voltage detection. Literature [4] proposes a control strategy which can realize frequency multiplication effects and two-way switch natural flow changing without detecting polarity of load current. This strategy overcomes the inherent problem of voltage and current overshoot in the converter and is easy to realize. As to the issue of inverter control, many experts and scholars have been conducting a lot of researches in recent years [5-17]. Combining with predictive current control, literature [5] works out the unique 27 vector current control method for converter based on the analysis of the influences of input voltage on output current. Literature [6] puts forward a strategy using three-level operation modulation instead of the former two-level matrix converter; the modulation strategy based on separation and link idea has been widely used in single-phase high frequency link inverter. For three-phase inverter, a large amount of simulation results have proved its practical application.

One of the important technical indicators for aviation power is efficiency and energy saving. A control strategy based on typology separation and link SPWM modulation is proposed in this paper, which has the basis in the new single-phase voltage loop control strategy in literature [14] which is based on resonant controller. Compared with the control strategy in literature [14], the proposed strategy has the advantages of two-way energy flow and low harmonic.

2. The idea of separation and link for high-frequency link inverter with matrix converter

The high-frequency link inverter with matrix converter is mainly composed of full bridge inverter (DC/AC), high-frequency transformer, matrix converter (AC1/AC2) and filter, as illustrated in Figure 1. DC voltage is modulated inversely into high-frequency voltage pulses by full-bridge inverter, high-frequency voltage pulses are isolated by high-frequency transformer and modulated by matrix converter to output sinusoidal voltage with industrial frequency through filter.

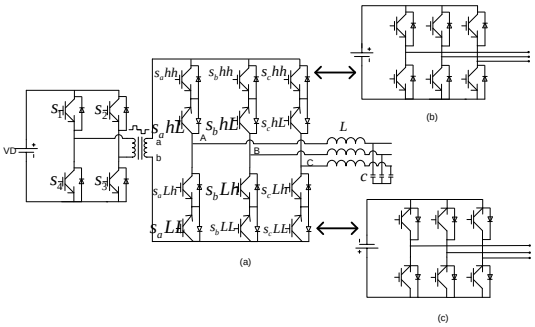

Figure 1. Structure of separation and link

The control of first-stage full-bridge inverter can adopt PWM control. The high-frequency transformer outputs high-frequency voltage pulses, as shown in Figure 2. From time 0 to t1, s1 and s3 can be conducted, the transformer outputs +VD. The second-stage matrix converter can be equivalent to that shown in Figure 1-b. Within t1-t2 and t3-t4, when the full-bridge inverter is changing phases, the inherent dead time exists in switches, the output voltage is 0 and the feed-back energy can be achieved by freewheeling diode. Within t2-t3, s2 and s4 can be conducted, the output voltage is –VD and second-stage matrix converter can be equivalent to that shown in Figure 2. The whole process is the main idea of separation and link.

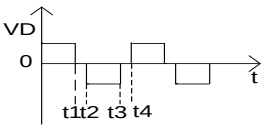

Figure 2. High-frequency voltage pulse

3. Studies on strategies of converting current for matrix converter

In the course of operation for matrix converter, two basic principles must be obeyed [17].

Any two random phases of inputs for matrix converter cannot be short circuit so as to avoid over current caused by short circuit of voltage source.

Any one random phase of outputs for matrix converter cannot be open circuit so as to protect inductive load from sudden open circuit and results in over voltage.

According to the principle, the single-phase/three-phase matrix converter has 12 kinds of working conditions, as shown in Table 1. In the table, the six conditions (+1, +2, +3 and -1, -2, -3) denote that the input of second-stage matrix converter is a positive voltage, the inverter b is in working condition and the inverter c does not work. Other six conditions (+4, +5, +6 and -4, -5, -6) express the input of second-stage matrix converter is a negative voltage, the inverter c is in working condition and the inverter b does not work. u_{ab} denotes the input voltage of matrix converter; u_{AB}, u_{BC} and u_{CA} represent respectively the output of line voltage for three-phase power.

Table 1. Working conditions of matrix converter

Conditions	u_{AB}	u_{BC}	u_{CA}	Conduction switch
+1	u_{ab}	0	$-u_{ab}$	$S_ahh\ S_bLh\ S_cLh$
-1	$-u_{ab}$	0	u_{ab}	$S_bhh\ S_chh\ S_aLh$
+2	$-u_{ab}$	u_{ab}	0	$S_bhh\ S_aLh\ S_cLh$
-2	u_{ab}	$-u_{ab}$	0	$S_ahh\ S_chh\ S_bLh$
+3	0	$-u_{ab}$	u_{ab}	$S_chh\ S_aLh\ S_bLh$
-3	0	u_{ab}	$-u_{ab}$	$S_ahh\ S_bhh\ S_cLh$
+4	u_{ab}	0	$-u_{ab}$	$S_aLL\ S_bhL\ S_chL$
-4	$-u_{ab}$	0	u_{ab}	$S_ahL\ S_cLL\ S_bLL$
+5	$-u_{ab}$	u_{ab}	0	$S_ahL\ S_chL\ S_bLL$
-5	u_{ab}	$-u_{ab}$	0	$S_bhL\ S_aLL$ S_bLL
+6	0	$-u_{ab}$	u_{ab}	$S_ahL\ S_bhL\ S_bLL$
-6	0	u_{ab}	$-u_{ab}$	$S_chL\ S_aLL$ S_bLL

According to the demand of output, different modulation strategies can be applied. After the logical combination of the above 12 switching conditions, the desired output voltage will be obtained.

SPWM based on the ideas of separation and link is that two decoupling inverters are respectively modulated by SPWM at first and then the driving signals of two inverters by SPWM are logically combined (shown in Figure 3), namely separation and link. After separation and link, the control signals control the switches of matrix converter. In Figure 4, the phase u has been taken as an example and the realization of 4 driving signals of switching above two-way bridge arm for matrix converter has been illustrated. The triangle waves u_r are the carrier waves and the sine waves u_c are two complementary SPWM signals after modulation and comparison. Then, the two SPWM signals and the square waves are logically computed to get four signals for controlling switches, and the square waves have the frequency of divide-by-2 carrier wave, the phase difference of 180o, of which the duty cycle is 0.5. Similarly, other phase control signals can be obtained.

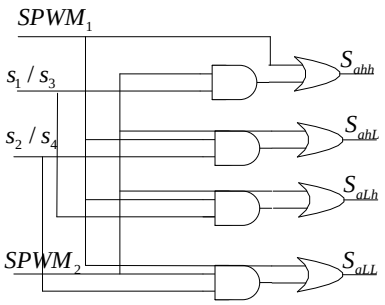

Figure 3. Logical combination

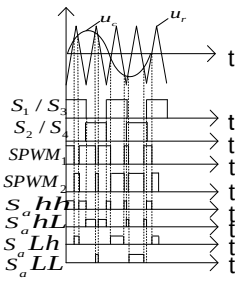

Figure 4. Switch signals of decoupling

4. Mathematical argumentation of topology with separation and link for matrix converter

4.1 Mathematical model of space state for matrix converter

From the above, the strategies of converting current of topology with separation and link for matrix converter have been theoretically analyzed. The mathematical model of space state of AC-AC matrix converter has been established in literature [18].

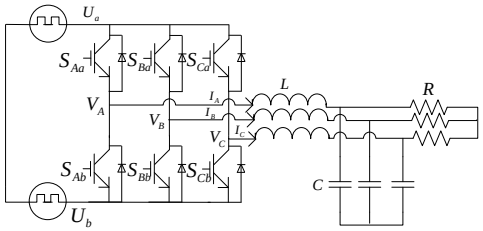

Figure 5. State model of switches

Define the switch function S_{jk} : $j \in \{A,B,C\}$, $k \in \{a,b\}$

$$\begin{cases} S_{jk}=1 & S_{jk} \text{ conducted} \\ S_{jk}=0 & S_{jk} \text{ open} \end{cases} \quad (1)$$

According to Figure 5, the space state Equation (15-16) can be listed:

$$\frac{d}{dt}\begin{bmatrix} I_A \\ I_B \\ I_C \\ V_A \\ V_B \\ V_C \end{bmatrix} = \begin{bmatrix} 0 & 0 & 0 & -\frac{1}{L} & 0 & 0 \\ 0 & 0 & 0 & 0 & -\frac{1}{L} & 0 \\ 0 & 0 & 0 & 0 & 0 & -\frac{1}{L} \\ \frac{1}{C} & 0 & 0 & -\frac{1}{RC} & 0 & 0 \\ 0 & \frac{1}{C} & 0 & 0 & 0 & 0 \\ 0 & 0 & \frac{1}{C} & 0 & 0 & -\frac{1}{RC} \end{bmatrix} \begin{bmatrix} I_A \\ I_B \\ I_C \\ V_A \\ V_B \\ V_C \end{bmatrix} + \frac{1}{L}\begin{bmatrix} S_{Aa} & S_{Ab} \\ S_{Ba} & S_{Bb} \\ S_{Ca} & S_{Cb} \\ 0 & 0 \\ 0 & 0 \\ 0 & 0 \end{bmatrix} \begin{bmatrix} U_a \\ U_b \end{bmatrix} \quad (2)$$

4.2 Switch model of three-phase inverter

The mathematical models have been established for conventional three-phase inverters in Figure 6.

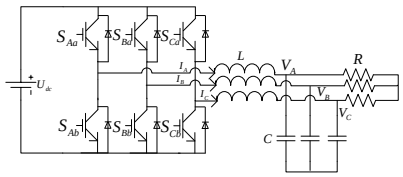

Figure 6. Switch model of conventional three-phase inverter

In light of Figure 6, the constraints of each switch on one bridge arm have been defined [19]: $S_{ia}+S_{ib}=1$, the switch function has been defined: $S_i = S_{ia} - S_{ib}$, $i \in \{A,B,C\}$, and the state equation is shown in Equation (3).

$$\frac{d}{dt}\begin{bmatrix} I_A \\ I_B \\ I_C \\ V_A \\ V_B \\ V_C \end{bmatrix} = \begin{bmatrix} 0 & 0 & 0 & -\frac{1}{L} & 0 & 0 \\ 0 & 0 & 0 & 0 & -\frac{1}{L} & 0 \\ 0 & 0 & 0 & 0 & 0 & -\frac{1}{L} \\ \frac{1}{C} & 0 & 0 & -\frac{1}{RC} & 0 & 0 \\ 0 & \frac{1}{C} & 0 & 0 & 0 & 0 \\ 0 & 0 & \frac{1}{C} & 0 & 0 & -\frac{1}{RC} \end{bmatrix} \begin{bmatrix} I_A \\ I_B \\ I_C \\ V_A \\ V_B \\ V_C \end{bmatrix} + \frac{1}{L}\begin{bmatrix} S_A \\ S_B \\ S_C \\ 0 \\ 0 \\ 0 \end{bmatrix} U_{dc} \quad (3)$$

4.3 Mathematical argumentation of separation and link

From Equation (4), which shows the input voltage of second-stage matrix of high-frequency link inverter, the topology of second-stage matrix convertor in Figure 1 can be completely equivalent to Figure 5.

$$\begin{cases} U_a = V_D \\ U_b = 0 \end{cases} (0 < t < \frac{2}{T}) \quad \begin{cases} U_a = 0 \\ U_b = V_d \end{cases} (\frac{2}{T} < t < T) \quad (4)$$

Substituting Equation (4) into state space Equation (2), the mathematical equations of high-frequency inverter with matrix converter can be achieved, shown in Equation (5), when $0 < t < \frac{2}{T}$ and in Equation (6), when $\frac{2}{T} < t < T$.

$$\frac{d}{dt}\begin{bmatrix} I_A \\ I_B \\ I_C \\ V_A \\ V_B \\ V_C \end{bmatrix} = \begin{bmatrix} 0 & 0 & 0 & -\frac{1}{L} & 0 & 0 \\ 0 & 0 & 0 & 0 & -\frac{1}{L} & 0 \\ 0 & 0 & 0 & 0 & 0 & -\frac{1}{L} \\ \frac{1}{C} & 0 & 0 & -\frac{1}{RC} & 0 & 0 \\ 0 & \frac{1}{C} & 0 & 0 & 0 & 0 \\ 0 & 0 & \frac{1}{C} & 0 & 0 & -\frac{1}{RC} \end{bmatrix} \begin{bmatrix} I_A \\ I_B \\ I_C \\ V_A \\ V_B \\ V_C \end{bmatrix} + \frac{1}{L}\begin{bmatrix} S_{Aa} & S_{Ab} \\ S_{Ba} & S_{Bb} \\ S_{Ca} & S_{Cb} \\ 0 & 0 \\ 0 & 0 \\ 0 & 0 \end{bmatrix} \begin{bmatrix} V_D \\ 0 \end{bmatrix} \quad (5)$$

$$\frac{d}{dt}\begin{bmatrix} I_A \\ I_B \\ I_C \\ V_A \\ V_B \\ V_C \end{bmatrix} = \begin{bmatrix} 0 & 0 & 0 & -\frac{1}{L} & 0 & 0 \\ 0 & 0 & 0 & 0 & -\frac{1}{L} & 0 \\ 0 & 0 & 0 & 0 & 0 & -\frac{1}{L} \\ \frac{1}{C} & 0 & 0 & -\frac{1}{RC} & 0 & 0 \\ 0 & \frac{1}{C} & 0 & 0 & 0 & 0 \\ 0 & 0 & \frac{1}{C} & 0 & 0 & -\frac{1}{RC} \end{bmatrix} \begin{bmatrix} I_A \\ I_B \\ I_C \\ V_A \\ V_B \\ V_C \end{bmatrix} + \frac{1}{L} \begin{bmatrix} S_{Aa} & S_{Ab} \\ S_{Ba} & S_{Bb} \\ S_{Ca} & S_{Cb} \\ 0 & 0 \\ 0 & 0 \\ 0 & 0 \end{bmatrix} \begin{bmatrix} 0 \\ V_D \end{bmatrix}$$

(6)

After the decoupling of matrix converter, the inverter input is shown in Equation (7).

$$\begin{cases} U_{dc} = V_D (0 < t < \frac{2}{T}) \\ U_{dc} = V_D (\frac{2}{T} < t < T) \end{cases} \quad (7)$$

Substituting Equation (5) into the mathematical Equation (3) of conventional inverter, the mathematical equations of separation and link of topology for high-frequency link inverter is shown in Equation (8) when $0 < t < \frac{2}{T}$ and in Equation (9) when $\frac{2}{T} < t < T$.

$$\frac{d}{dt}\begin{bmatrix} I_A \\ I_B \\ I_C \\ V_A \\ V_B \\ V_C \end{bmatrix} = \begin{bmatrix} 0 & 0 & 0 & -\frac{1}{L} & 0 & 0 \\ 0 & 0 & 0 & 0 & -\frac{1}{L} & 0 \\ 0 & 0 & 0 & 0 & 0 & -\frac{1}{L} \\ \frac{1}{C} & 0 & 0 & -\frac{1}{RC} & 0 & 0 \\ 0 & \frac{1}{C} & 0 & 0 & 0 & 0 \\ 0 & 0 & \frac{1}{C} & 0 & 0 & -\frac{1}{RC} \end{bmatrix} \begin{bmatrix} I_A \\ I_B \\ I_C \\ V_A \\ V_B \\ V_C \end{bmatrix} + \frac{1}{L} \begin{bmatrix} S_A \\ S_B \\ S_C \\ 0 \\ 0 \\ 0 \end{bmatrix} V_D$$

(8)

$$\frac{d}{dt}\begin{bmatrix} I_A \\ I_B \\ I_C \\ V_A \\ V_B \\ V_C \end{bmatrix} = \begin{bmatrix} 0 & 0 & 0 & -\frac{1}{L} & 0 & 0 \\ 0 & 0 & 0 & 0 & -\frac{1}{L} & 0 \\ 0 & 0 & 0 & 0 & 0 & -\frac{1}{L} \\ \frac{1}{C} & 0 & 0 & -\frac{1}{RC} & 0 & 0 \\ 0 & \frac{1}{C} & 0 & 0 & 0 & 0 \\ 0 & 0 & \frac{1}{C} & 0 & 0 & -\frac{1}{RC} \end{bmatrix} \begin{bmatrix} I_A \\ I_B \\ I_C \\ V_A \\ V_B \\ V_C \end{bmatrix} + \frac{1}{L} \begin{bmatrix} S_A \\ S_B \\ S_C \\ 0 \\ 0 \\ 0 \end{bmatrix} (-V_D)$$

(9)

From $S_i = S_{ia} - S_{ib}$, it is known that Equation (10) and Equation (11) are workable.

$$\begin{bmatrix} S_A \\ S_B \\ S_C \\ 0 \\ 0 \\ 0 \end{bmatrix} V_D = \begin{bmatrix} S_{Aa} & S_{Ab} \\ S_{Ba} & S_{Bb} \\ S_{Ca} & S_{Cb} \\ 0 & 0 \\ 0 & 0 \\ 0 & 0 \end{bmatrix} \begin{bmatrix} V_D \\ 0 \end{bmatrix} \quad (10)$$

$$\begin{bmatrix} S_A \\ S_B \\ S_C \\ 0 \\ 0 \\ 0 \end{bmatrix} (-V_D) = \begin{bmatrix} S_{Aa} & S_{Ab} \\ S_{Ba} & S_{Bb} \\ S_{Ca} & S_{Cb} \\ 0 & 0 \\ 0 & 0 \\ 0 & 0 \end{bmatrix} \begin{bmatrix} 0 \\ V_D \end{bmatrix} \quad (11)$$

From the above mathematical derivation, it is deduced that the mathematical model of space state of matrix converter is completely equivalent to the model of separation and link of topology of matrix converter, namely, the control strategy of separation and link of topology of matrix converter has been proved to be valid.

5. Simulations and experimental analysis

The proposed control strategy in Figure 1 has been simulated and studied from experiments. The parameters in simulation are set as follows: the DC voltage is 25V, the frequency of full-bridge switch is 10 KHz, the switch frequency of matrix converter is 20 KHz, the modulation ratio m=0.8, the ratio of transformer turn $n_1 : n_2$ =1:1, the filter inductance L = 0.3mH, the filtering capacitor C = 33 μF, the resistive load R = 100 Ω.

5.1 Simulation analysis

Figure 7 shows the simulation of switching signals of full-bridge inverter, and Figure 8 is the theoretical two switching signals for u-phase, Figure 9 shows the theoretical waveforms of u_{AB}, u_{BC} line voltage for u-phase before filtering. From the simulated waveform, it can be found that the control strategy proposed in this article has better control effects. There are no obvious overshoot signals before and after voltage waveform, ideal switching effects are achieved.

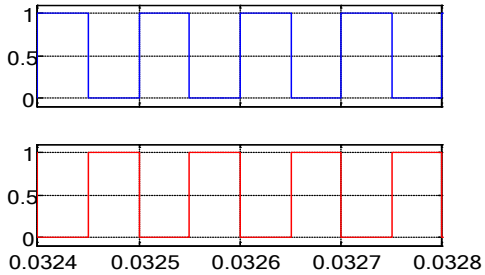

Figure 7. Simulation of switching signals of full-bridge inverter

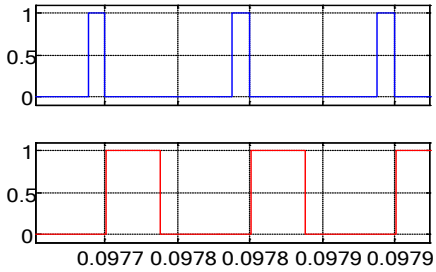

Figure 8. Simulation of $S_{ahh}S_{ahl}$ switching signal of phase u

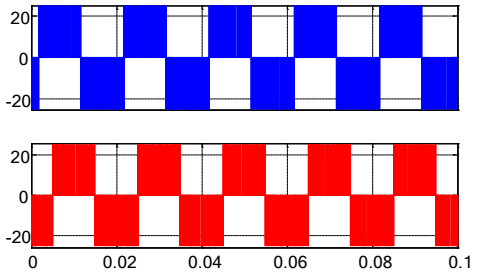

Figure 9. Simulation of u_{AB}、u_{BC} line voltage

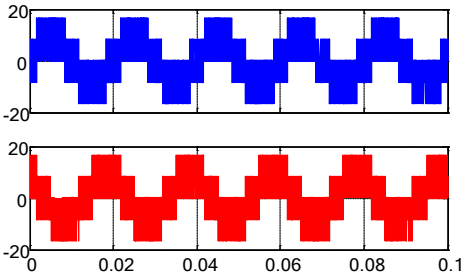

Figure 10. Simulation u_A, u_B phase voltage measurement

Experimental verification

According to the control strategy in Figure 1, three SPWM signals with phase difference of 120° and two PWM signals with phase difference of 180° which are produced by TMS320F2812 are selected, the input three SPWM signals and two PWM signals are logically operated by EPM240T100C5N, and 12 switch signals are produced, the experimental verification platform is shown in Figure 12.

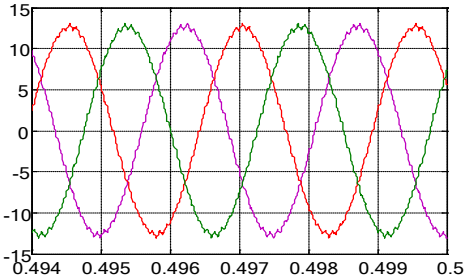

Figure 11. The u_A, u_B, u_C phase voltage after filtering

The timer of DSP produces 2 PWM signals to control the chip of photoelectric coupling isolation TLP250 and receive the driving signal with 15V to further control MOSFET, driving signals of full-bridge inverter in the experiment are shown in Figure 13. From the comparison between Figure 7 and 13, the theoretical switching signals have the same frequency and phase with the driving signals in the experiment, the subsequent requirements of the experiment can be fully met.

After the CPLD Boolean calculation of two PWM signals and three SPWM signals, the 12 switch signals of the second-stage matrix converter are obtained. Figure 14 shows the two switch signals of phase u after logic calculation. From the comparison between Figure 8 and Figure 14, the theoretical values

are completely the same as the experimental values.

Figure 15 shows u_{AB}, u_{BC} waveforms of line voltage before filtering. From Figure 9, although the data from the experiment do not achieve the ideal state, other data of voltage waveforms are not affected.

Figure 16 shows u_A, u_B phase voltage waveforms before filtering, From Figure 10, it can be found that there is some difference between the actual result and the theoretical state. The reason is that the matrix converter needs 6 ways of isolation power supply and the electromagnetism interference among isolation powers exists. During the process of changing phases for matrix converter, the nonlinear actions of switches have an impact on the laboratory equipment. Thus, the interference occurs in the experiments.

Figure 17 shows u_A, u_B phase voltage waveforms after filtering. Under the condition of 12V/50Hz and THD=6.6425%, the voltage waveforms are sinusoidal. Although there is dead time during MOSFET switching, distortion appears in the voltage waveforms, but they can completely meet the performance requirements.

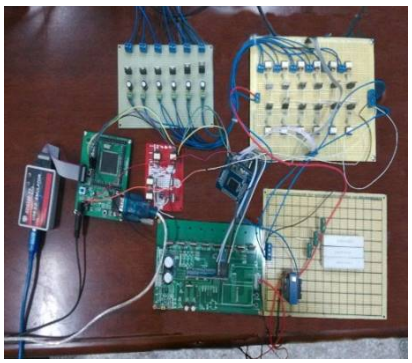

Figure 12. A screenshot of the experimental verification platform

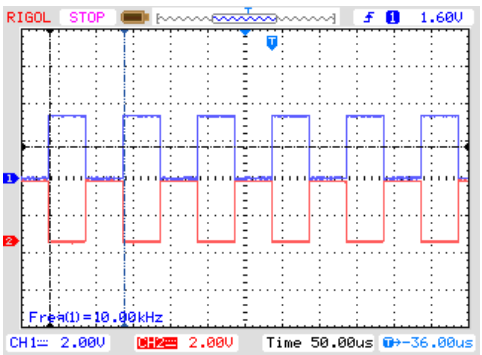

Figure 13. Experiment of driving signals of full-bridge inverter

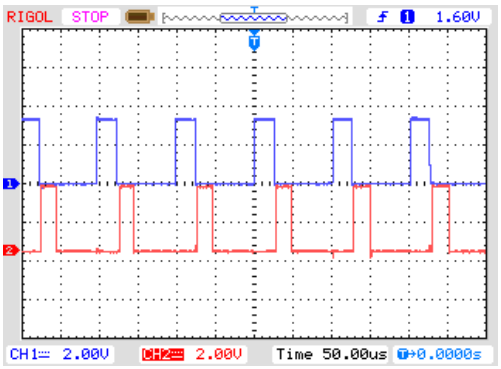

Figure 14. $S_{ahh}S_{ahl}$ drive signals of phase u

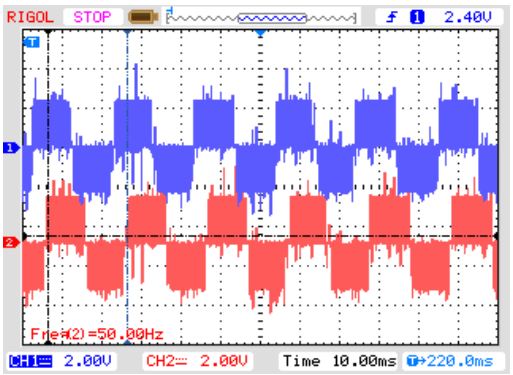

Figure 15. u_{AB}. u_{BC} line voltage

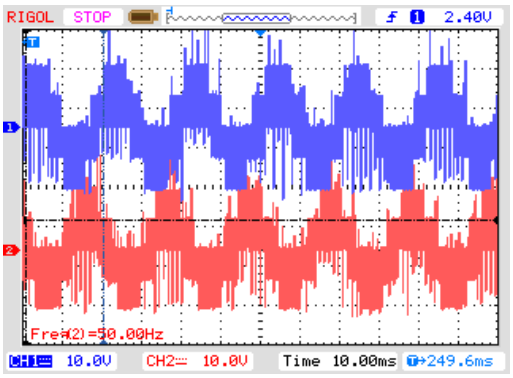

Figure 16. u_A, u_B phase voltage

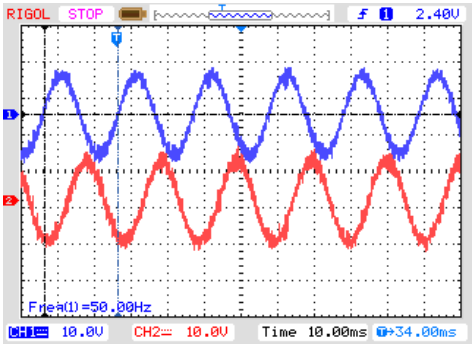

Figure 17. u_A, u_B phase voltage after filtering

6. Conclusions

Matrix converter is the core part of high-frequency link inverter with matrix

convertor, so a control strategy of SPWM of separation and link of topology for matrix convertor has been proposed and the detailed mathematical argumentation has been provided in the paper. The single-phase/three-phase matrix converter is decoupled into two conventional three-phase inverters for controlling. Then, the driving signals of SPWM of the two converters are logically combined into 12 switch signals, thus the control strategy for the conventional three-phase inverter is introduced into matrix converter.

Compared with traditional strategies of converting current, it is much easier to understand the strategy of converting current of matrix converter from the aspect of separation and link of topology. The control process is simple and easy to implement. Through simulation and experiments, the validity of this control strategy has been verified, it is believed that this strategy can provide some reference to high-frequency link inverter with matrix convertor for further study.

References

1. Wu Shenghua, Zhong Yanping, Lai Xiangdong, et al. (2013) Improvement of Control Strategy for Matrix Sinusoid-al Converter with High Frequency Link. *Transactions of China Electrotechnical Society*. 28(3), p. p. 228-233.
2. Espelage PM, Bose BK. (1997) High Frequency Link Power Conversion. *IEEE Transactions on Industry Applications*. 13(5), p.p. 387-394.
3. Mei Yang, Sun Kai, Huang Lipei (2007) Three-Phase to Single-Phase Matrix Converter Using RB-IGBT. *Transactions of China Electrotechnical Society*. 22(3), p.p. 91-95.
4. Wu Shenghua, Quan Jianzhou, Lai Xiangdong, et al.(2013) Research of New Three-phase Sinusoidal Converters Based on Matrix Converters With the High Frequency Link. *Proceedings of the CSEE*. 33(6), p.p. 25-30.
5. Ma Zhixue, Ma Hao (2004) Current Control Strategies for Matrix Converter. *Proceedings of the CSEE*. 24(8), p.p. 61-66.
6. Li Lijuan, Zhu Jianlin, Liu Hongliang (2008) Topology and Control Strategy of Three-Level Matrix Converter. *Electric Power Automation Equipment*. 28(3), p.p. 63-67.
7. Cai Wei, Zhang Xiaofeng, Qiao Mingzhong, et al. (2013) Comparison between Two Modulation Methods of Matrix Converter. *Power System Protection and Control*. 41(10), p.p. 111-117.
8. Nashiren FM. (2009) Neutral-point-clamped Multilevel Inverter Using Space Vevtor Modulation. *European Journal of Scientific Research*. 28(1), p.p. 82-91.
9. Lee MY. *Three-level Neutral-point-clamped Matrix Converter Topology*. Nottingham University: Nottingham, England. 2009; 1-10.
10. Ma Xinghe, Tan Guojun, Wang Xudong, et al. (2009) An Improved Two Line Voltage Synthesis Control Strategy of Matrix Converter. *Transactions of China Electrotechnical Society*. 24(4), p.p.126-138.
11. Zheng Lianqing, Huang Jinbo (2012) Research on Integration SPWM Strategy for Three-phase Inverter Based on High Frequency Linked Matrix Converter. *Journal of North China Electric Power University*. 39(2), p.p. 8-11.
12. Li Lijuan, Wang Feng, Yi Lingzhi, et al. (2013) Equivalent Circuit and Its Applications for Multilevel Matrix Converter. *High Voltage Engineering*. 39(3), p.p. 741-748.
13. Li Zixin, Wang Ping, Li Yaohua, et al. 400 Hz High-power Voltage-source Inverter with Digital Control. *Proceedings of the CSEE*. 2009; 29(6): 36-42.
14. Yan Zhaoyang, Zhang Chunjiang, Wu Weiyang, et al. (2012) De-Re-Couple SPWM Strategy for Single-Phase High-Frequency Link Matrix Inverter. *Transactions of China Electrotechnical Society*. 27(2), p.p. 50-67.
15. Yan Zhaoyang, Jia Minli, Zhang Chunjiang, et al. (2010) Principle and Realization of HPWM Strategy for Three-Phase Inverter Based on High

Frequency Linked Matrix Converter. *Transactions of China Electrotechnical Society*. 25(11), p. p. 113-121.
16. Han Pengwu, Zhang Daisheng,Wang Siming (2013) Research of Bipolarity Phase-Shifted Controlled High Frequency Link Inverter with Matrix Converter. *Low Voltage Apparatus*. (13), p.p. 33-37.
17. Wu Shenghua, Zheng Bo, Liu Xiao (2014) Improvement on Control Strategy for Matrix AC/DC Converter. *Journal of Air Force Early Warning Academy*. 28(1), p.p. 48-51.
18. Li Houchun, Ge Hongjuan, Zhang Wenbin, et al. (2013) Research and Implementation of a Novel Three-phase to Single-phase Matrix Converter. *Power Electronics*. 47(3), p.p. 90-92.
19. GuoYi, Dong Rong, Feng Long (2013) Research and Simulation on Over-Modulation Method of Matrix Converter. *Telecom Power Technology*. 4(30), p.p.11-15.
20. Zheng Xueqin, Tang Ningping (2001) The analysis of AC-AC matrix converter equivalent circuit. *Journal of Fuzhou University (Natural Science)*. (1), p.p. 39-42.